Phase Transition and Elastic Properties of Zinc Sulfide Under High Pressure from First Principles Calculations

Dai Wei[a,c], Song Jin-Fan[b], Wang Ping[b], Lu Cheng[b], Lu Zhi-Wen[b], and Tan Xiao-Ming[d]

[a] Department of Physics and Electronics, Hubei University of Education, Wuhan 430205, China
[b] Department of Physics, Nanyang Normal University, Nanyang 473061, China
[c] Institute of Fluid Physics, Chinese Academy of Engineering Physics, Mianyang 621900, China
[d] Department of Physics, Ludong University, Yantai 264025, China

Reprint requests to L. C.; E-mail: lucheng@nynu.edu.cn

Z. Naturforsch. **66a,** 656 – 660 (2011) / DOI: 10.5560/ZNA.2011-0033
Received April 14, 2011 / revised July 4, 2011

A theoretical investigation on structural and elastic properties of zinc sulfide semiconductor under high pressure is performed by employing the first-principles method based on the density functional theory. The calculated results show that the transition pressure P_t for the structural phase transition from the B3 structure to the B1 structure is 17.04 GPa. The calculated values are generally speaking in good agreement with experiments and with similar theoretical calculations.

Key words: High Pressure; Structural Transition; Zinc Sulfide.

1. Introduction

Zinc sulfide (ZnS), an important direct band gap (3.66 eV at 300 K) II – VI compound semiconductor, is of great interest because of its wide range of technological applications in electroluminescent devices, infrared windows, sensors, and lasers, etc [1]. The structural properties and phase stabilities of ZnS semiconductors are of considerable importance, particularly in high-pressure science. High pressure experiments on ZnS provide valuable data, which help to formulate fundamental concepts on the physical properties of semiconductor materials. A fascinating problem is the structural change and its phase transitions as a reaction on the external pressure. With the rapid development of high pressure techniques, extensive experimental works have been done to address the high pressure behaviour of ZnS in the past few years [2 – 8]. The pressure induced phase transitions of ZnS from the zincblende (ZB) structure to the rocksalt (RS) structure was first reported as 24.0 GPa by Samara and Drickamer [3]. Baars and Brandt presented X-ray diffraction structural measurements on the ZnS semiconductor and investigated the structural phase transitions in ZnS between 20 and 1200 °C [4]. On the basis of the X-ray diffraction through a diamond anvil cell, Zhou et al. measured the equation of state and optical properties for the high pressure phase of ZnS at room temperature. They reported that the structural phase transition pressure value was 15 GPa [5].

Theoretically, the investigations of the high pressure behaviour of ZnS have made remarkable progress by using the ab initio method [9 – 11]. Chen et al. investigated the phase transition of ZnS from the ZB structure to the RS structure by the ab initio plane-wave pseudopotential density functional theory method and found that the pressures for the transition from the ZB structure to the RS structure are 17.5 GPa from total energy–volume data and 15.4 GPa from equal enthalpies [9]. Gupta et al. performed a theoretical study of the structural phase transformation of ZnS under high pressure using first principle plane wave pseudopotential (PW-PP) and full potential linear augmented plane wave (FPLAPW) method [11]. Bilge et al. calculated the B3 – B1 phase transition and mechanical properties of ZnS and predicted that the phase transition from the B3 structure to the B1 structure occurs at a pressure of 18.5 GPa [10]. However, comparing with the availability of precise experimental date, an adequate analysis of the microscopic physical origin of ZnS under high pressure is still lacking, especially for the elastic properties of both phases.

© 2011 Verlag der Zeitschrift für Naturforschung, Tübingen · http://znaturforsch.com

In this paper, we describe a systematical investigation of the high pressure behaviour and structural phase transition of ZnS by first-principles quantum-mechanical calculations. Our original motivation for this work is threefold. Firstly, it is to give a comprehensive and complementary investigation of the structural and elastic properties of ZnS in ZB and RS structure under high pressure. Our second intention is to provide a reasonable interpretation about the structural phase transition between B1 phase and B3 phase of ZnS. We are motivated, thirdly, by the hope that such an investigation might contribute some further understanding of the thermodynamic properties of ZnS and its related semiconductor materials.

2. Theory

The thermodynamic state of a solid system is usually defined by pressure, volume, and temperature, linked by the equation of state. Generally, the simplest isothermal equation of state for solids is given by the definition of the bulk modulus B [12],

$$B = -\frac{\mathrm{d}P}{\mathrm{d}\ln V}\,. \tag{1}$$

This simple equation of state is obviously not suitable for high pressures since it does not take into account the fact that it is more and more difficult to compress the solid, i.e. that the bulk modulus increases with pressure. In this work, the third-order Birch–Murnaghan equation of state has been used for fitting the theoretical data since it is most often used in experimental studies of solids at high pressure. The third-order Birch–Murnaghan equation of state can be written as [12]

$$\begin{aligned} P = {} & \frac{3}{2}B_0\left[\left(\frac{V_0}{V}\right)^{7/3} - \left(\frac{V_0}{V}\right)^{5/3}\right] \\ & \cdot\left\{1+\frac{3}{4}\left(B_0'-4\right)\left[\left(\frac{V_0}{V}\right)^{2/3}-1\right]\right\}. \end{aligned} \tag{2}$$

For a cubic crystal, there are three independent elastic constants (C_{11}, C_{12}, and C_{44}) which are believed to be related to the second-order change in the internal energy of a crystal under deformation. Hence, to investigate the stability of ZnS semiconductors, we have calculated the elastic constants under hydrostatic pressure by a direct method. In this method, the elastic constants are defined by means of a Taylor expansion of the total energy $E(V,\delta)$ for the system with respect to a small strain δ of the lattice primitive cell volume V. The energy of a strained system can be expressed as [13–17]

$$\begin{aligned} E(V,\delta) = {} & E(V_0,0) \\ & + V_0\left[\sum_i \tau_i\xi_i\delta_i + \frac{1}{2}\sum_{ij} C_{ij}\delta_i\xi_j\delta_j\right], \end{aligned} \tag{3}$$

where $E(V_0,0)$ is the energy of the unstrained system with equilibrium volume V_0, τ_i is an element in the stress tensor, and ξ_i is a factor to take care of the Voigt index. For the calculations of the elastic constants, we consider three independent volume-non-conserving strains [14–16]

$$\hat{\varepsilon}_1 = \begin{pmatrix} \delta & 0 & 0 \\ 0 & 0 & 0 \\ 0 & 0 & 0 \end{pmatrix},\ \hat{\varepsilon}_2 = \begin{pmatrix} 0 & 0 & 0 \\ 0 & \delta & 0 \\ 0 & 0 & 0 \end{pmatrix},\ \hat{\varepsilon}_3 = \begin{pmatrix} 0 & \delta & \delta \\ \delta & 0 & \delta \\ \delta & \delta & 0 \end{pmatrix}, \tag{4}$$

where $\hat{\varepsilon}_1$, $\hat{\varepsilon}_2$, and $\hat{\varepsilon}_3$ are the matrixes for the calculation of C_{11}, C_{12}, and C_{44}, respectively. The elastic constants C_{11}, C_{12}, and C_{44} can be defined as

$$C_{11} = \frac{1}{V}\frac{\partial^2 E(V,\hat{\varepsilon}_1)}{\partial\delta^2}\Big|_{\delta=0}\,, \tag{5}$$

$$C_{12} = \frac{1}{V}\frac{\partial^2 E(V,\hat{\varepsilon}_1)}{\partial\delta^2}\Big|_{\delta=0} - \frac{1}{2V}\frac{\partial^2 E(V,\hat{\varepsilon}_2)}{\partial\delta^2}\Big|_{\delta=0}\,, \tag{6}$$

$$C_{44} = \frac{1}{12V}\frac{\partial^2 E(V,\hat{\varepsilon}_3)}{\partial\delta^2}\Big|_{\delta=0}\,. \tag{7}$$

Under hydrostatic compression, in order to compare with experimental results, the elastic constants C_{ij} must be transformed into the observable elastic constants c_{ij} defined with respect to the finite strain variables. The three non-independent elastic constants (c_{11}, c_{12}, and c_{44}) can be transform into the three independent elastic constants (C_{11}, C_{12}, and C_{44}) as follows:

$$c_{11} = C_{11},\ \ c_{12} = C_{12} + P,\ \ c_{44} = C_{44} - \frac{P}{2}. \tag{8}$$

For a ZnS semiconductor, the stiffness and compliance constants are related by [17]

$$\begin{aligned} S_{11} &= \frac{1}{3}\left(\frac{1}{C_{11}+2C_{12}} + \frac{2}{C_{11}-C_{12}}\right), \\ S_{12} &= \frac{1}{3}\left(\frac{1}{C_{11}+2C_{12}} - \frac{1}{C_{11}-C_{12}}\right),\ \ S_{44} = \frac{1}{C_{44}}. \end{aligned} \tag{9}$$

3. Details of the Calculations

The first-principles calculations are performed using the pseudopotential plane-wave method, as implemented in the Cambridge serial total energy package (CASTEP) program [18, 19], which has been shown to yield reliable results for the electronic and structural properties of various solids. For structural property calculations, the exchange correlation potential is described in the generalized gradient approximation (GGA) using the Perdew–Burke–Ernzerhof (PBE) functional [20, 21]. The electronic wave functions are expanded in a plane-wave basis set with a cutoff energy of 650 eV for ZnS at zero and high pressure studies. Coulomb potential energy caused by electron–ion interaction is described in which orbital of Zn $3d^{10}\,4s^2$ and S $3s^2\,3p^4$ are treated as valence electrons. The special points sampling integration over the Brillouin zone are carried out using the Monkhorst–Pack method with a $20\times20\times20$ special k-point mesh. The tolerances for geometry optimization are set as the difference in total energy being within 10^{-6} eV/atom. The accuracy of the total energies obtained within the framework of density functional theory is in many cases sufficient to predict which structure at a given pressure has lowest free energy.

4. Results and Discussions

For both B1 and B3 phases of ZnS crystals, the first step in calculating the structural properties has been to find the equation of state. In order to establish the validity of the parameters used in the present investigation, we calculated the total energy of both B1-type and B3-type ZnS for a set of volumes. From the ground-state volume, we can find that the bulk modulus is a function of the volume (Fig. 1). From Figure 1, we can also confirm that the bulk modulus decrease rapidly with increasing volume. In order to fully exploit simple semiconductor materials, it is necessary to obtain a good understanding of ZnS, and in particular, its high pressure structural phase transition. The structural phase transition from the B3 phase to the B1 phase of ZnS is investigated at 0 K because of the simplicity of the calculations and because these phase changes are experimentally known to exhibit very little temperature dependence. In general, the free energy G can be expressed as [12]

$$G = E + PV - TS, \tag{10}$$

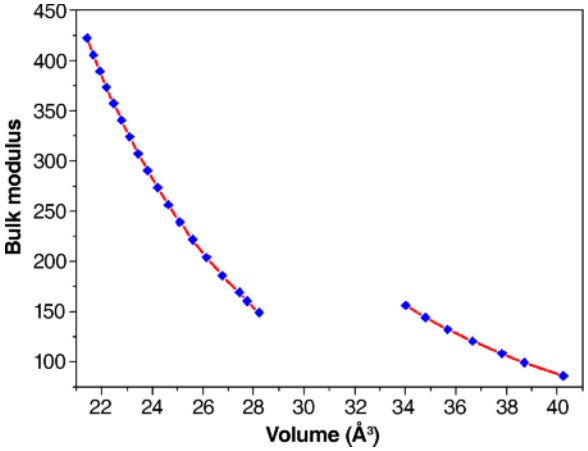

Fig. 1 (colour online). Dependence of bulk modulus on the cell volume of ZnS semiconductor.

where E is the internal energy, S the vibrational entropy, P the pressure, and V the volume. At $T = 0$ K, the Gibb's free energy G becomes equal to the enthalpy H [12]:

$$H = E + PV. \tag{11}$$

Under compression, the calculation shows that ZnS will undergo a structural phase transition from the B3 phase to the B1 phase by increasing the pressure, as shown in Figure 2. We calculated the total energy of ZnS in both the B3 structure and the B1 structure as a function of pressure from 0 to 100 GPa. The transition pressure P_t for the structural phase transitions is determined by the usual condition of equal enthalpies in the both phases, i.e. $H_{B1}(P_t) = H_{B2}(P_t)$. The variations of the enthalpy versus the pressure are presented in Figure 3. It is worth pointing out that the intersec-

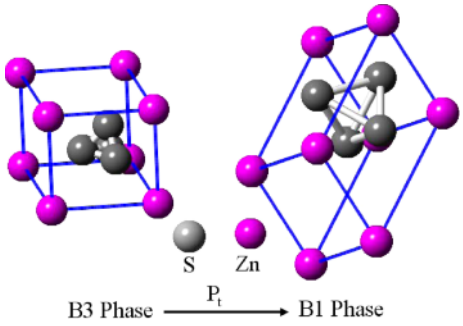

Fig. 2 (colour online). Crystal structures of ZnS in the two phase; left figure shows the zincblende (ZB) structure; right figure shows the rocksalt (RS) structure.

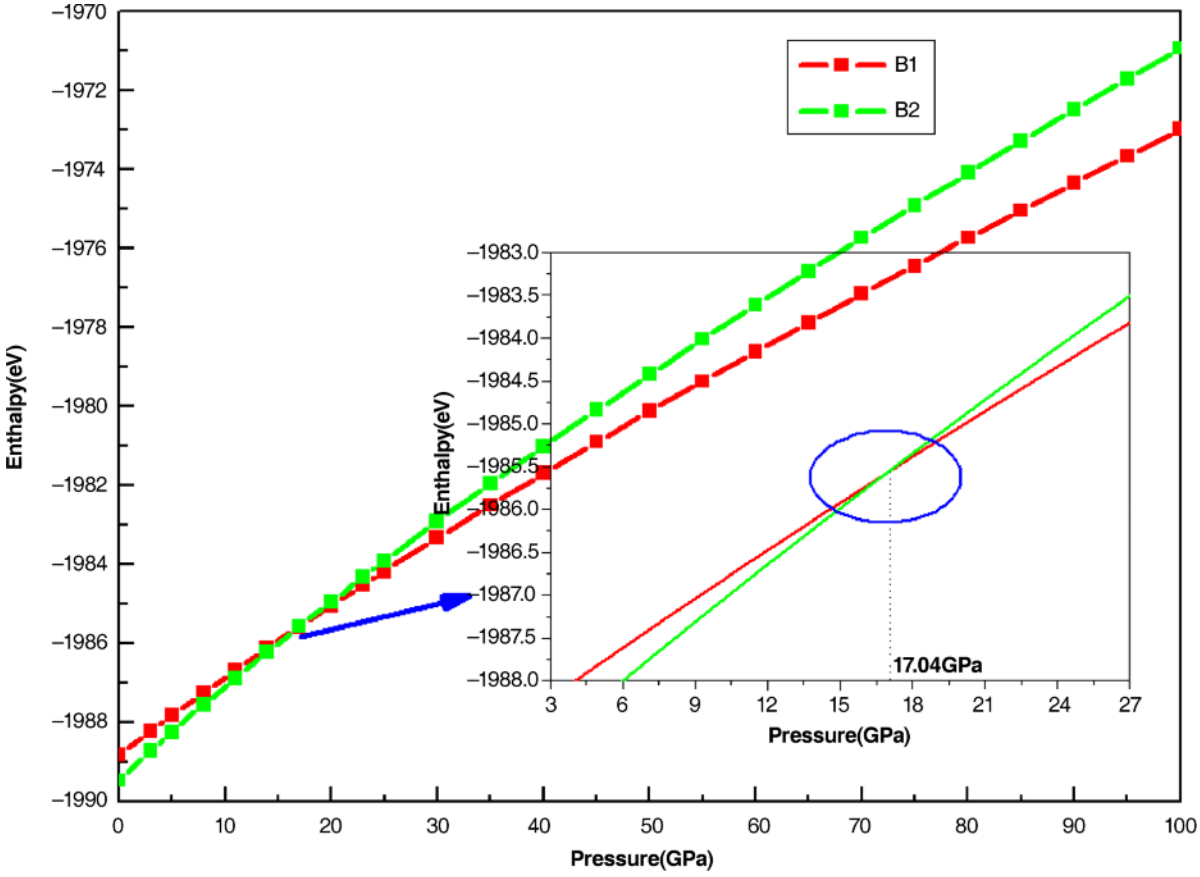

Fig. 3 (colour online). Enthalpy as a function of pressure for the B3 and B1 phases of ZnS.

tion of the two enthalpy curves implies that the B3 – B1 phase transition in ZnS occurs at 17.04 GPa. This result is in good agreement with experimental data [5] and theoretical work [9, 10].

Valuable information about the structural properties is very important for understanding the solid properties from a microscopic point of view. The reason is that the structural properties can provide highly detailed information about the nature of interatomic binding forces in solids. Using the first-principles calculations, we have calculated the structural properties for both B3-type and B1-type ZnS. The calculated lattice constant a, the primitive cell volume V_0, the bulk modulus B_0 for B1 and B3 phases are listed in Table 1, together with the available experimental and theoretical work for comparison. From Table 1, we can see that the calculated lattice constant a agree well with the experimental data. The overestimation of lattice constant a parameters is about 0.8% for B1 phase and 0.5% for B3 phase. The good agreement between them shows the accuracy of the present electronic structure calculations. To gain further insight into the mechanical stability of ZnS crystals, we have calculated the elastic

Table 1. Calculated and experimental lattice constant [Å], primitive cell volume [Å^3], bulk modulus [GPa] of ZnS at zero pressure.

Structure		a	V_0	B_0
B3	Present work	5.440	40.239	69.533
	Experiment [6]	5.410		76.900
	Experiment [7]			78.000
	Theory [9]	5.404		71.220
	Theory [10]	5.449		70.020
B1	Present work	5.099	33.148	86.380
	Experiment [5]	5.130		85.000
	Experiment [8]	5.060		103.60
	Theory [9]	5.070		89.540
	Theory [10]	5.107		85.107

Table 2. Calculated and experimental elastic stiffness constants C_{ij} [GPa] and elastic compliance constants S_{ij} [1/GPa] for ZnS at zero pressure.

Structure		C_{11}	C_{12}	C_{44}	S_{11}	S_{12}	S_{44}
B3	Present work	96.9	48.3	55.8	0.0178067	−0.0065064	0.0206949
	Theory [9]	99.6	57.0	50.5			
	Theory [10]	97.2	56.4	64.1			
	Experiment [7]	104.0	65.0	46.2			
B1	Present work	123.5	49.1	67.8	0.0132328	−0.0046869	0.0203684
	Theory [9]	136.1	65.0	54.1			
	Theory [10]	133.1	61.1	47.1			

constants using the ab initio stress–strain relations. The theoretical results are given in Table 2.

5. Conclusions

Using the pseudopotential plane-waves method based on the density functional theory, within the generalized gradient approximation, we studied the structural and elastic properties of ZnS semiconductor under high pressure. From the theoretical calculation, the structural phase transition of ZnS from the B3 phase to the B1 phase is determined. The calculated results are found to be in good agreement with the available experimental data and theoretical values. Unfortunately, as far as we know, there are no experimental data available related to the elastic properties of B1-type ZnS in the literature for our comparison. Hence, careful experimental investigations are required in order to clarify the elastic properties of B1-type ZnS in detail.

Acknowledgement

This work was supported by the Natural Science Foundation of Henan Province (No. 102300410209), Natural Science Foundation of the Education Department, Henan Province (No. 2011B140015), Natural Science Foundation of the Education Department, Hubei Province (No. B20113002), and Nanyan Normal University Science Foundation (No. zx20100011).

[1] Y. C. Zhu, Y. Bando, D. F. Xue, and D. Golberg, J. Am. Chem. Soc. **125**, 16196 (2003).
[2] Z. P. Li, B. B. Liu, S. D. Yu, J. H. Wang, Q. J. Li, B. Zou, T. Cui, Z. X. Liu, Z. Q. Chen, and J. Liu, J. Phys. Chem. C **115**, 357 (2011).
[3] G. A. Samara and H. G. Drickamer, J. Phys. Chem. Solids **23**, 457 (1962).
[4] J. Baars and G. Brandt, J. Phys. Chem. Solids **34**, 905 (1973).
[5] Y. H. Zhou, A. J. Campbell, and D. L. Heinz, J. Phys. Chem. Solids **52**, 821 (1991).
[6] O. Madelung, Numerical Data and Functional Relationships in Science and Technology, Springer-Verlag, Berlin 1982.
[7] D. Berlincourt, H. Jaffe, and L. R. Shiozawa, Phys. Rev. **129**, 1009 (1963).
[8] S. Ves, U. Schwarz, N. E. Christensen, K. Syassen, and M. Cardona, Phys. Rev. B **42**, 9113 (1990).
[9] X. R. Chen, X. F. Li, C. L. Cai, and J. Zhu, Solid State Commun. **139**, 246 (2006).
[10] M. Bilge, S. Özdemir Kart, H. H. Kart, and T. Çağın, Mater. Chem. Phys. **111**, 559 (2008).
[11] S. K. Gupta, S. Kumar, and S. Auluck, Optics Commun. **284**, 20 (2011).
[12] J. P. Poirier, Introduction to the Physics of the Earth's Interior, Cambridge University Press, Cambridge, UK 2000.
[13] G. V. Sin'ko, Phys. Rev. B **77**, 104118 (2008).
[14] S. Özdemir Kart, M. Uludoğan, I. Karaman, and T. Çağın, Phys. Stat. Sol. (a) **205**, 1026 (2008).
[15] M. Kalay, H. H. Kart, S. Özdemir Kart, and T. Çağın, J. Alloys Compd. **484**, 431 (2009).
[16] T. Tsuchiya and K. Kawamura, J. Chem. Phys. **114**, 10086 (2001).
[17] S. Özdemir Kart and T. Çağın, J. Alloys Compd. **508**, 177 (2010).
[18] M. D. Segall, P. L. D. Lindan, M. J. Probert, C. J. Pickard, P. J. Hasnip, S. J. Clark, and M. C. Payne, J. Phys.: Cond. Matt. **14**, 2717 (2002).
[19] S. J. Clark, M. D. Segall, C. J. Pickard, P. J. Hasnip, M. J. Probert, K. Refson, and M. C. Payne, Z. Kristallogr. **220**, 567 (2005).
[20] J. P. Perdew, K. Burke, and M. Ernzerhof, Phys. Rev. Lett. **77**, 3865 (1996).
[21] J. P. Perdew, S. Kurth, A. Zupan, and B. Peter, Phys. Rev. Lett. **82**, 2544 (1999).